Available online at www.sciencedirect.com
SCIENCE DIRECT
Polymer 47 (2006) 3049–3056
polymer
www.elsevier.com/locate/polymer

The synthesis and characterization of polystyrene/magnetic polyhedral oligomeric silsesquioxane (POSS) nanocomposites

Xiao Yan Song [a,b,c], Hai Ping Geng [a,b,c], Qi Fang Li [a,b,c,*]

[a] College of Material Science and Engineering, Beijing University of Chemical Technology, Beijing, China
[b] Key Laboratory for Nano-Materials, Ministry of Education, Beijing, China
[c] Key Laboratory on Preparation and Processing of Novel Polymer Materials of Beijing, Beijing, China

Received 26 October 2005; received in revised form 4 January 2006; accepted 19 February 2006
Available online 20 March 2006

Abstract

Fc–CH=CH–C_6H_6–$(C_5H_9)_7Si_8O_{12}$ (POSS1, Fc: ferrocene) which contain both metal and C=C double bond was firstly synthesized by Wittig reaction. The chemical structure of POSS1 was characterized by FTIR, ^1H, ^{13}C and ^{29}Si NMR, mass spectrometry and elemental analysis, and the magnetic property of POSS1 have also been studied. Polystyrene composites containing inorganic–organic hybrid polyhedral oligomeric silsesquioxane (POSS1) were prepared by bulk free radical polymerization. XRD and TEM studies indicate that POSS1 is completely dispersed at molecular level in PS matrix when 1 wt% POSS1 is introduced, while some POSS1-rich nanoparticals are present when content of POSS1 is beyond 3 wt%. GPC results show that molecular weight of the PS/POSS1 nanocomposites are increased with addition of POSS1. TGA and TMA data show the thermal stabilities of PS/POSS1 nanocomposites have been improved compared to neat PS. The PS/POSS1 nanocomposites also display higher glass transition temperatures (T_g) in comparison with neat PS. Viscoelastic properties of PS/POSS1 nanocomposites were investigated by DMTA. The results show the storage modulus (E') values (temperature $> T_g$) and the loss factor peak values of the PS/POSS1 nanocomposites are higher than that of neat PS. Mechanical properties of the PS/POSS1 nanocomposites are improved compared to the neat PS.

Keywords: Polyhedral oligomeric silsesquioxane (POSS); Ferrocene; Nanocomposites

1. Introduction

The development of organic–inorganic nanocomposites with improved properties has attracted much interest in past few years [1–5]. Organic–inorganic nanocomposites materials have been regarded as new generation of high performance materials since they combine the advantages of the inorganic materials (rigidity, high stability) and the organic polymers (flexibility, dielectric, ductility and processibility). Clays as typical non-ofillers have been extensively used as reinforcement agents to prepare polymer-layered silicate nonocomposites with improved thermal and mechanical properties [6–12]. The efficiency of the clays to modify the properties of the polymer is primarily determined by the degree of its dispersion in the polymer matrix. But in the past few years, much attention has been paid to the silsesquioxanes $(RSiO_{1.5})_8$ with specific cage structures for their symmetry. These polyhedral oligomeric silsesquioxanes (POSS) offer a unique opportunity for preparing organic–inorganic hybrid materials with the inorganic phase truly molecularly dispersed in the nanocomposites [13–24], owing to their organic or inorganic substituent [25]. POSS macromers have an inorganic silica-like core and are surrounded by eight organic groups, of which eight or one is generally reactive. These reactive corner groups include styryl [3–5], methacrylate [13,14], norbornyl [15–17], vinyl [18,19], epoxy [20–22], siloxane [23], nitriles [24], amines [24] and so on. These functional POSS molecules are generally used for synthesis of copolymers, which display enhanced properties.

In recent years numerous transition metal and lanthanide silsesquioxane complexes [26–29] used as model for heterogeneous silica-supported transition metal catalysts have been prepared. Preparation and characterization of a variety of iron containing POMSS compounds have been studied [30,31]. Ferrocenyl and permethylferrocenyl polymers containing cyclic and polyhedral silsesquioxanes as frameworks have been prepared via the hydrosilylation reaction of vinylferrocene and octasilsesquioxane or cyclosiloxanes [32–34]. Kenji Wada [35] synthesized a series of metallocene containing

* Corresponding author. Tel.: +86 10 64421693
E-mail address: qflee@mail.buct.edu.cn (Q.F. Li).

0032-3861/$ - see front matter © 2006 Elsevier Ltd. All rights reserved.
doi:10.1016/j.polymer.2006.02.055

silsesquioxane bearing functional groups with partial cage structures. But up to now, symmetrical POSS compounds with cage structures, which contain both metal and functional group have not been reported. These POSS compounds with magnetic property could be copolymerized with olefin under controlled magnetic field and the effect of magnetic field on the tacticity of the copolymers will be studied very soon.

The monofunctional styryl-POSS monomers, $[R_7(Si_8O_{12})(-CH_2CH_2C_6H_4CH{=}CH_2)]$ (R: c-C_6H_{11} or c-C_5H_9) have already been used to modify polymethylstyrene by copolymerization with methyl styrene [3,4]. The T_g values of copolymers were lower than that of neat polymethylstrene when content of styryl-POSS monomer was less than 9 mol% [3]. The viscoelastic behavior of these copolymers presented a rubber-like behavior at high temperature when POSS mole fraction increased to 8 mol% [4]. The multifunctional styryl-POSS had also been used to improve the thermal properties and storage modulus of copolymers [5]. However, the effect of the POSS on the mechanical properties of PS was seldom studied, and little research has appeared on the use of non-functional POSS with ferrocene.

In this paper, styrylcyclopentyl-POSS monomer with ferrocene (POSS1) was first synthesized by Wittig reaction and used to prepare PS/POSS1 nanocomposites with the same free radical initiation condition as PS, and their viscoelastic, thermal and mechanical properties were also studied.

2. Experimental

2.1. Materials and preparation of samples

4-Chlorobenzyltrichlorosilane and cyclopentyltrichlorosilane were supplied by Aldrich. ferrocenecarboxaldehyde was obtained from Acros. Styrene and 2,2′-azobis (isobutyronitrile) were supplied from Beijing reagent corporation, Beijing, China. All reactions were carried out under an atmosphere of dry nitrogen. Solvents were dried over calcium hydroxide and freshly distilled prior to use.

2.1.1. Preparation of 4-chlorobenzylcyclopentyl-POSS

A slight excess of 4-chlorobenzyltrichlorosilane (0.74 g) was slowly added to a 60 ml dry tetrahydrofurane (THF) solution of $(C_5H_9)_7Si_7O_9(OH)_3$ (2.36 g) and pyridine (1.2 ml). The reaction occurred rapidly upon mixing, as an evidence of the precipitation of pyridine hydrochloride. The reaction solution was stirred at 0 °C for 0.5 h, and then rose to room temperature for 4 h, followed by filtration to remove the pyridine hydrochloride byproduct. The solution of product was concentrated to 5 ml and then was added to rapidly stirred acetone (50 ml). The precipitated product was collected on a buchner funnel and washed with acetone and distilled water, and then dried in vacuo to yield 2 g 4-chlorobenzylcyclopentyl-POSS (90% yield).

^{1}H NMR ($CDCl_3$, 600 MHz, δ ppm): 7.66(d, 2H, J= 7.80 Hz, H-2 and H-6), 7.39(d, 2H, J=7.80 Hz, H-3 and H-5), 4.58(s, 2H, CH_2Cl), 0.97–1.74(63H, cyclopentyl). ^{13}C NMR ($DCCl_3$): 139.2(C-1), 134.5(2C, C-2, and C-6), 132.5(C-4), 127.7(2C, C-3 and C-5), 46.1(1C, CH_2Cl), 22.2–27.3(35C, cyclopentyl). IR (KBr, cm^{-1}): Si–O–Si(1108), 2950–2865(–CH_2–, cyclopentyl) 1608(C–H, benzene), 1398(H–C–H, methyl) 913(C–C, benzene).

2.1.2. Preparation of benzylcyclopentyl-POSS triphenylphosphonium chloride

1.41 g (5 mmol) triphenylphosphine was added to a solution of 5.48 g (5 mmol) 4-chlorobenzylcyclopentyl-POSS in 20 ml of anhydrous toluene and then was heated at the reflux temperature overnight to give a white solid that was filtered and washed with toluene. 6.54 g (96%).

^{1}H NMR ($CDCl_3$, 600 MHz, δ ppm): 7.747(m, 9H, $P(Ph)_3$), 7.611(s, 6H, $P(Ph)_3$), 7.407(d, 2H, J=7.20 Hz, H-2 and H-6), 7.079(d, 2H, J=7.20 Hz, H-3 and H-5), 5.537(d, 2H, –CH_2P), 0.955–1.734(63H, cyclopentyl). IR (KBr, cm^{-1}): Si–O–Si(1111), 2950–2865(–CH_2–, cyclopentyl) 1608(C–H, benzene), 1398(H–C–H, methyl), 913(C–C, benzene), 1439(P–Ph).

2.1.3. Preparation of POSS1

In a three-necked bottom flask placed in an ice-water bath, was placed benzylcyclopentyl-POSS triphenylphosphonium chloride (1.3 g, 1 mmol) dissolved in anhydrous chloroform (15 ml), After 30 min, followed by dropwise addition of 1.2 mmol of sodium ethoxide into the solution. After 1.5 h, the mixture was stirred for 20 h at room temperature, then 2 ml of 2% HCl were added into the solution, and the resulting mixture was extracted with chloroform. The organic layers were combined, washed with distilled water and brine for three times, respectively, dried over $MgSO_4$, filtered and concentrated in vacuum to give the crude products. Crude product was purified by silica gel column chromatography using *n*-hexane/dichloromethane (10:1) as eluent to give a mixture of 48% (*E*)- and 52% (*Z*)-stereoisomers which were calculated by ^{1}H NMR. Pure product was orange solid (1.06 g, 89%).

2.1.3.1. (E)-POSS1. ^{1}H NMR ($CDCl_3$, 600 MHz, δ ppm): 7.614 (d, 2H, J=7.800 Hz, H-3′ and H-5′), 7.412(d, 2H, J= 7.800 Hz, H-2′ and H-6′), 6.928(d, 1H, J=16.20 Hz, H-1), 6.651(d, 1H, J=16.20 Hz, H-2), 4.493(s, 2H, H-2″ and H-5″), 4.311(s, 2H, H-3″ and H-4″), 4.149(s, 5H, cyclopentadienyl), 0.972–1.747(63H, cyclopentyl). ^{13}C NMR ($DCCl_3$): 134.4 (2C, C-3′ and C-5′), 125.0(2C, C-2′ and C-6′), 139.5(C-1′), 130.4(C-4′), 128.4(C-1), 126.0(C-2), 82.5(C-1″), 69.4(7C, C-3″, C-4″ and 5C, cyclopentadienyl), 67.0(2C, C-2″ and C-5″), 27.3(14C, cyclopentyl), 27.0(14C, cyclopentyl), 22.6(7C, cyclopentyl). ^{29}Si NMR ($DCCl_3$): −66.15, −66.49, −79.62. IR (KBr, cm^{-1}): Si–O–Si(1109), 2950–2866(–CH_2–, cyclopentyl), 1600(C–H, benzene), 913(C–C, benzene) 1634 (C=C), 958(–*CH*=*CH*–), 1600(C–H, benzene), 806(C–H, benzene). MALDI-TOF MS: M^+(1186). Anal. Found: C, 52.98%; H, 6.668%. Calc.: C, 53.60%; H, 6.580%.

2.1.3.2. (Z)-POSS1. ^{1}H NMR ($CDCl_3$, 600 MHz, δ ppm): 7.572 (d, 2H, J=7.800 Hz, H-3′ and H-5′), 7.333(d, 2H, J= 7.800 Hz, H-2′ and H-6′), 6.408(d, 1H, J=12.00 Hz, H-1),

6.314(d, 1H, $J=16.20$ Hz, H-2), 4.186(s, 4H, H-2″ and H-5″, H-3″ and H-4″), 4.095(s, 5H, cyclopentadienyl), 0.972–1.747 (63H, cyclopentyl). ^{13}C NMR ($DCCl_3$): 133.8(2C, C-3′ and C-5′), 140.1(C-1′), 127.9(2C, C-2′and C-6′), 128.6(C-1), 127.1(C-2), 130.2(C-4′), 80.5(C-1″), 69.6(2C, C-3″ and C-4″), 69.4(5C, cyclopentadienyl), 68.7(2C, C-2″ and C-5″), 27.3(14C, cyclopentyl), 27.0(14C, cyclopentyl), 22.6(7C, cyclopentyl). ^{29}Si NMR ($DCCl_3$): −66.15, −66.49, −79.62. IR (KBr, cm^{-1}): Si–O–Si(1109), 1600(C–H, benzene), 2950–2866(–CH_2–, cyclopentyl), 913(C–C, benzene), 1634(C=C), 850(–*CH=CH*–), 1600(C–H, benzene), 806(C–H, benzene). MALDI-TOF MS: M^+(1186). Anal. Found: C, 52.98%; H, 6.680%. Calc.: C, 53.60%; H, 6.620%.

2.1.4. Preparation of PS/POSS1 nanocomposites

One weight percent POSS1 was dissolved into styrene and heated to 80 °C under an atmosphere of dry nitrogen, then 1 wt% 2,2′-azobis (isobutyronitrile) employed as the initiator was added into it. These mixtures were magnetically stirred at 80 °C for 2 h and then were put into a mold followed by being cured at 80 °C for 16 h. PS1 nanocomposite with 1 wt% POSS1 was prepared. When 0, 3 and 5 wt% POSS1 were added into stryrene, respectively, PS0, PS3 and PS5 were prepared employing the condition equivalent with that of PS1. PS0, PS1, PS3 and PS5 were all transparent.

2.2. Measurements

NMR spectrometer were recorded on a Brucher av600 NMR Spectrometer (^{1}H 600 MHz, ^{13}C 150 MHz, ^{29}Si 119 MHz). Chemical shifts are reported in ppm and referenced to residual solvent resonances (^{1}H, ^{13}C) or an internal standard (^{1}H, ^{29}Si: TMS = 0 ppm). Infrared spectroscopic measurements were performed in the range 4000–400 cm^{-1} at a resolution of 1.0 cm^{-1} using a Brucher Tensor 27 FTIR Spectrometer. MALDI-TOF MS was recorded on a BRUKER BIFLEX III mass spectrograph. Elemental analyses were performed using Carlo Erba 1106. The magnetic properties were measured on Vibrating Sample Susceptibility System Model JDM-13.

XRD measurements were performed to examine the potential POSS alteration of the solid-state polymer microstructure in the PS/POSS nanocomposites. XRD can probe ordered POSS aggregates formed by phase separation. The samples were examined with a D/Max2500 VB2+/PC X-ray diffractometer. Scans were taken over the 2θ range of 2–40° with a step size of 0.03° at 1 s per step. A H800 transmission electron microscope (HITACHI JAP, INC.) was used to characterize the phase morphology in the PS/POSS1 nanocomposites. The samples were ultromicrotomed to 70–90 nm thickness and mounted on Cu TEM grids. The GPC-equipment used was Waters 515–2410 with three columns (10^3, 10^5, 10^6 Å), THF was used as solvent, the temperature was 30 °C and the flow-rate 1 ml/min.

The thermal properties of these hybrids were determined by thermal gravimetric analysis (TGA), Differential scanning calorimetry (DSC) and thermo mechanical analysis. TGA was carried out using a TG 209 C thermogravimetric analyzer operated at a heating rate of 10 °C/min from room temperature to 600 °C under a continuous flow of nitrogen. The calorimetric measurement was performed on a NETZSCH DSC 200PC thermal analysis apparatus at a heating rate of 10 °C/min in a dry nitrogen atmosphere. The glass transition temperatures were taken as the midpoint of the capacity change. In all the measurements, T_g was taken from the second scans. Thermo-mechanical analysis (TMA) was done in a TMA 202 C from NETZSCH Instruments Inc at a heating rate of 2 °C/min in a dry nitrogen atmosphere. Dynamic mechanical thermal analysis (DTMA) measurements were performed using a DMA Rheometric Scientific V in a single cantilever bending mode over a temperature range from 50 to 180 °C. Heating rate and frequency were fixed at 2 °C/min and 1 Hz, respectively. Tensile tests were carried out on an Instron-1121 tester with crosshead speed of 5 mm/min at room temperature. The specimen dimensions were scaled to ASTM D638M-II norm dimensions. Impact test was also carried out based on ISO 180/1U, by using a RESIL CEAST impact tester.

3. Result and discussion

3.1. Synthesis of POSS1

The synthetic route to POSS1 was outlined in Scheme 1. The incompletely condensed silsesquioxane (cyclo-$C_5H_9)_7$-$Si_7O_9(OH)_3$ was prepared in good yield by Feher's method

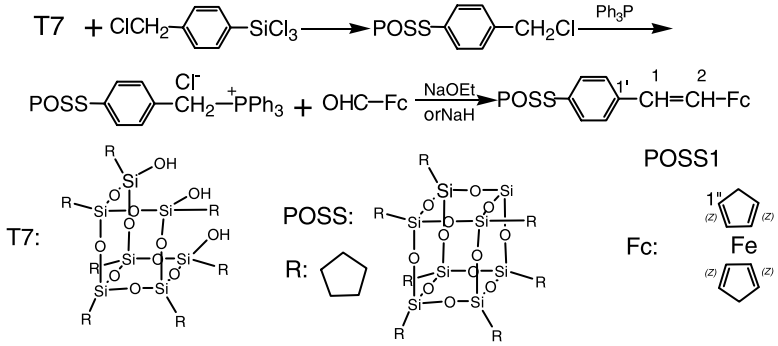

Scheme 1.

[36]. The reaction between (cyclo-$C_5H_9)_7Si_7O_9(OH)_3$, 4-chlorobenzyl trichlorosilane and excess pyridine in dry THF gave the corner-capped product, 4-chlorobenzylcyclopentyl-POSS which reacted with triphenylphosphine to produce the benzylcyclopentyl-POSS triphenylphosphonium chloride. The salt was transformed to the benzylcyclopentyl-POSS triphenylphosphonium ylid in situ, which was treated with ferrocenecarboxaldehyde to give the POSS1 as a mixture of *E*- and *Z*-isomers by Wittig reaction. The yield of reaction depends on sequence of addition of ferrocenecarboxaldehyde and base, and nature of base. When ferrocenecarboxaldehyde was firstly added to the solution of benzylcyclopentyl-POSS triphenylphosphonium chloride in chloroform and then sodium ethoxide was added, good yield was given in contrasted to first addition of sodium ethoxide. The yield of POSS1 was 38% (*E*/*Z*=1:1, calculated by ^{1}H NMR) and 89% (*E*/*Z*=4:1), respectively when NaH and NaOEt was used as base.

3.2. Magnetic characterization of the POSS1

The magnetic field dependence of magnetization curve of POSS1 at 298 K is shown in Fig. 1. It can be observed that magnetization of POSS1 increases with magnetic field intensity linearly, which show the POSS1 exhibits paramagnetic properties at room temperature, and with a remnant magnetization of 0.035 emu/g. It is worth noting that hysteresis coercive force (H_c) of POSS1 is 0 Oe. It indicates that POSS1 presents ideal soft magnetic properties.

3.3. FTIR analysis of PS nanocomposites

Fig. 2 shows FTIR spectra of the neat PS and PS/POSS1 hybrid composites. The band near 1100 cm^{-1}, peak of the Si–O–Si bond, indicates that POSS1 is present in PS matrix. The intensities of this band in these hybrid composites are increased with POSS1 content, and narrowing of this band indicates that the POSS1 environment for hybrid composites is more homogeneous [37].

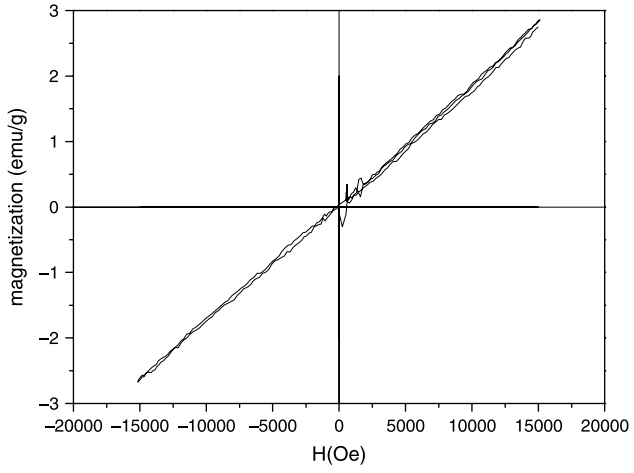

Fig. 1. Magnetization curves at room temperature for POSS1.

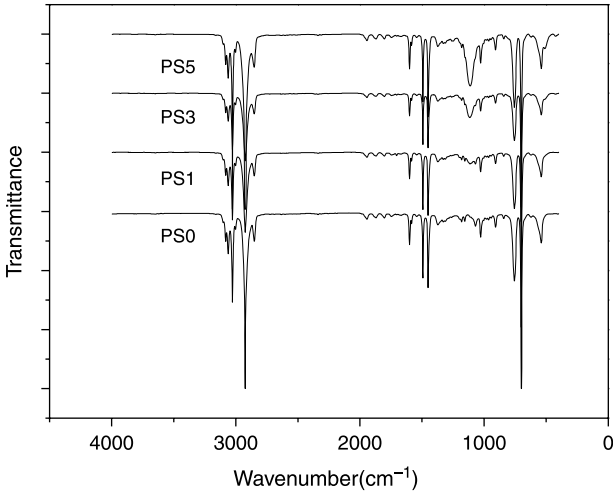

Fig. 2. IR spectra of the neat PS and PS/POSS1 nanocomposites.

3.4. Morphology of the nanocomposites

POSS1 was completely dissolved in styrene to form transparent solution. When 1 and 3 wt% amount of POSS1 were added into styrene, curing velocity of hybrid composites is slightly faster than that of neat PS, but beyond 5 wt% POSS1, curing velocity of hybrid composites is so slow that hybrid composites are not completely cured after 24 h. This indicates that a few POSS1 maybe make for polymerization of styrene and big volume POSS1 aggregated in the PS matrix, which is observed by TEM can retard collision between the styrene molecules as POSS1 content increase, which can explain effect of POSS1 on molecular weight of PS.

Fig. 3 displays wide-angle X-ray diffraction (WAXRD) patterns for the neat PS and PS/POSS1 nanocomposites with compositions of 99/1, 97/3 and 95/5 (w/w). For comparison, the diffraction pattern of POSS1 is also shown. All crystalline peaks of POSS1 are absent from the diffraction pattern of PS1, but a small crystalline peak at approximately 8.2° (equivalent to an interplanar spacing of 1.08 nm) of POSS1 is present in PS3 and PS5. This implies that there is no separated POSS1

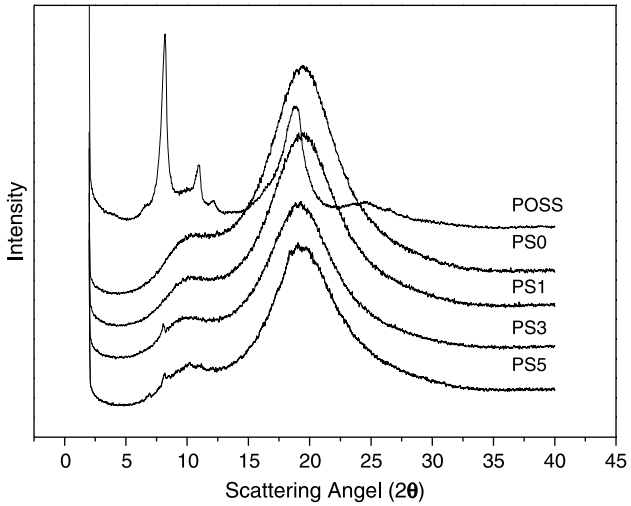

Fig. 3. XRD patterns of the pure PS and PS/POSS1 nanocomposites.

phase dispersed in PS1 nanocomposites and POSS1 can copolymerize with styrene to form homogeneous composites, but one fraction of POSS1 is aggregated in PS when POSS1 content is beyond 3%. The amorphous peak at 19.4° in the diffraction patterns of PS/POSS1 nanocomposites is closed to the amorphous peak of the pure PS, but the presence of aggregated crystal POSS1 results in the asymmetry increase in the amorphous peak progressively with increasing POSS1 content.

TEM micrographs of homogeneous are shown in Fig. 4, in which POSS1 is dispersed in the PS matrix. TEM micrographs of PS1 show no apparent evidence for the presence of POSS1 aggregates. Fig. 4(a) shows that some POSS1 particles in the PS3 are presented in stripe shape. In the PS5, besides stripe shape POSS1, some aggregated POSS1 particles from about 50 to 300 nm in diameter can be observed by Fig. 4(b). This indicates that POSS1 has been molecularly existed in the PS1 composites, and some POSS1 particles is blended with PS in the PS3 and PS5 in agreement with XRD studies, but POSS1 in the PS3 is better dispersed than that in the PS5.

3.5. Effect of POSS1 on molecular weight of PS

Despite the uncertainty caused by use of the polystyrene standards, GPC was a useful tool to qualitatively evaluate the size of polymer molecules and their distribution. GPC column retention time vs. concentration curves are plotted in Fig. 5. All curves have an overlapping peak between 17 and 25 min, and a small peak at 31 min in PS3 and PS5 nanocomposites in agreement with that of POSS. These show that a fraction of POSS1 is not copolymerized with styrene for large steric hindrance and blended with PS in PS3 and PS5 nanocomposites, corresponding to XRD and TEM results. Average molecular weights of PS/POSS1 nanocomposites determined by GPC are listed in Table 1. Molecular weights of PS increase after adding POSS1. After addition of 1 wt% POSS1, weight-average molecular weight is higher 8000 than that of the neat PS, but up to 5 wt%, average molecular weight decreases as much as the neat PS. M_w/M_n ratios, indexes of relative breadths

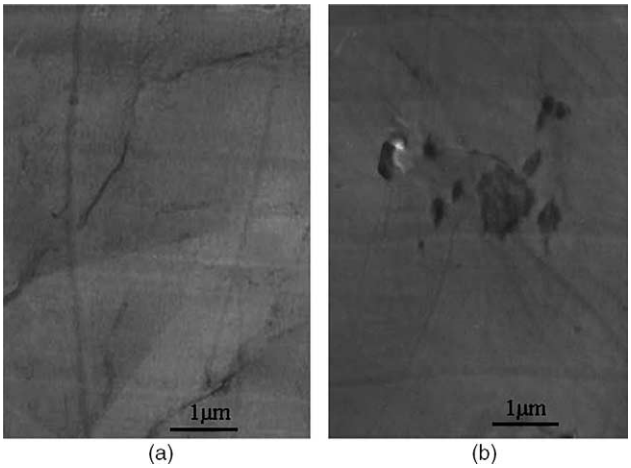

Fig. 4. TEM micrographs of the PS3 (a) and PS5 (b).

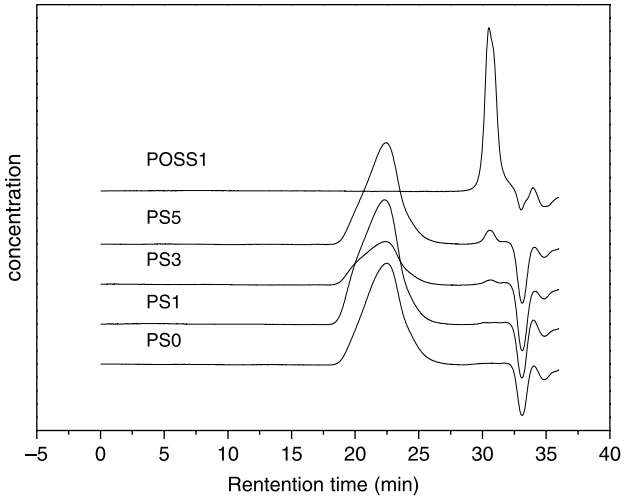

Fig. 5. GPC retention time vs. concentration curves.

of the molecular weight distributions have no apparent difference.

3.6. Thermal properties

Thermo-gravimetric curves of PS and hybrid composites are shown in Fig. 6 under nitrogen at ramp rate of 10 °C/min. The initial decomposed temperature of PS is improved with increase of POSS1 content, and that of PS0, PS1, PS3 and PS5 are 392.9, 401.8, 404.9 and 409.8 °C, respectively. It is clearly shown in Fig. 6 that the thermal stability of PS3 is the best at the whole temperature region.

The thermal deformation behavior of PS/POSS1 nanocomposites with the temperature along the *Z*-axis measured by TMA at ramp rate of 2 °C/min are shown in Fig. 7. In the TMA experiment, 30 N stress was placed on the surface of samples. Fig. 7 shows there is no thermal changes at an initial region, then is followed by a non-linear behavior which is the main deformation region, and curves present a level off region with constant deformation with increasing temperature at final stage. It can be seen that the temperature of initial deformation are 77.5, 77.6, 84.1, and 84.8 °C, respectively for PS0, PS1, PS3 and PS5. The percentage deformation of PS0, PS1, PS3 and PS5 are 10.22, 8.14, 5.51 and 5.71%, respectively at 120 °C, and 34.79, 19.22, 11.56 and 27.81%, respectively in the level off region.

The improvements in the thermal stability of hybrid composites can be resulted from the strong interaction between the polystyrene and the POSS1 macromolecules and the inherent good thermal stability of the POSS1. Molecule weights of hybrid composites also play an important role in

Table 1
Molecular weights of PS and PS/POSS1 nanocomposites

Polymer	M_n	M_w	PDI (M_w/M_n)
PS0	116,301	342,787	2.947
PS1	144,396	421,178	2.917
PS3	138,530	411,583	2.971
PS5	126,381	353,629	2.798

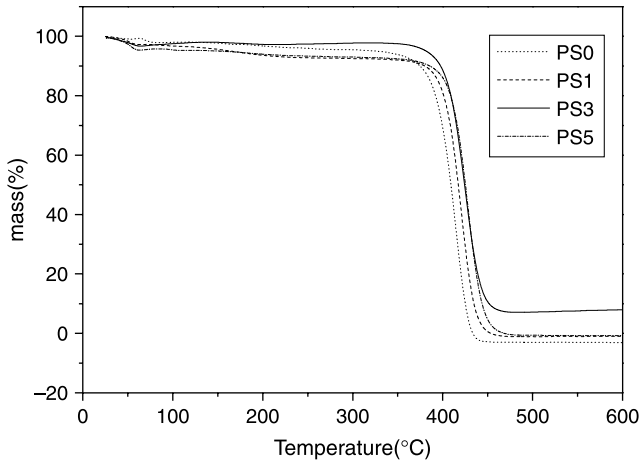

Fig. 6. Effect of POSS1 contents on the thermal stability of PS/POSS1 nanocomposites.

the thermal stability. All these effect factors result in the best thermal stability in PS3 nanocomposites.

3.7. Glass transition behavior

The DSC curves of pure polystyrene and the hybrids are presented in Fig. 8. All DSC thermograms display single glass transition temperatures in the experimental temperature range. It should be pointed out that the single glass transition erroneously indicate the hybrids are homogeneous since T_g of POSS1-rich phases can not be measured due to the high crystallinity of the POSS1 and thus the observed glass transition is attributed to polystyrene matrices. It is seen from Fig. 8 that addition of 3 wt% POSS1 shift T_g of PS towards a higher value by 10 °C and the hybrids containing 1 and 5 wt% of POSS1 have quite close glass transition temperature to PS3. Comparing these data to that obtained from Lei Zheng [38], it can be seen that T_g improvement for PS/POSS1 nanocomposites is better than that obtained for syndiotactic PS/POSS. Hadded and Lichtenhan [3] have reported that T_g of the hybrid increased by 10 °C when 1.1 mol% POSS is added, while only 3 wt% (0.27 mol%) POSS1 is added in our experiment. For

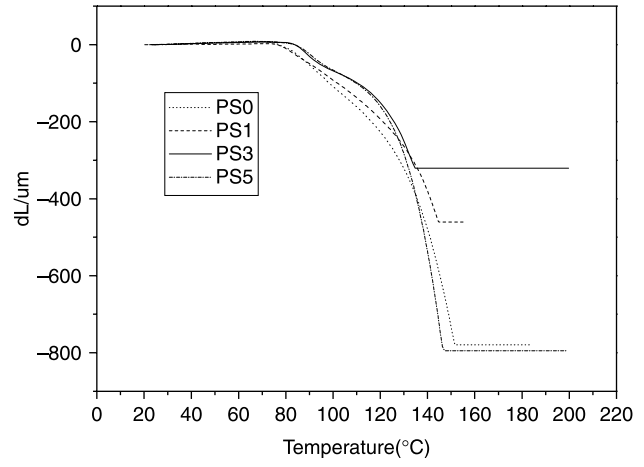

Fig. 7. The TMA thermograms for the neat PS and PS/POSS1 nanocomposites.

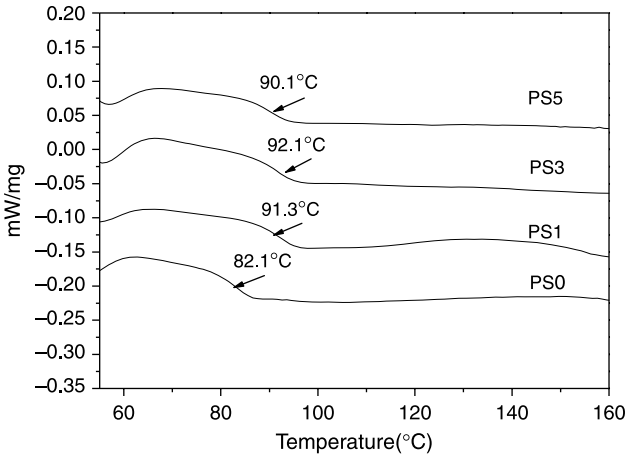

Fig. 8. The DSC curves of the pure PS and PS/POSS1 nanocomposites.

traditional PS/clay nonocomposites [7–9], few of their T_g is increased by more than 10 °C. POSS–clay (POSS–treated clay) was introduced into styrene to prepare PS/POSS–clay nonocomposites whose T_g value was 8 °C higher than the neat PS by Ding-Ru Yei [9].

Following earlier studies on organic/inorganic composites [39], films [40] and polymer/POSS nanocomposites [41], the improvements in the T_g of hybrid composites are likely to result from physical and chemical interactions as well as steric hindrances imposed by the inorganic phase to the molecular dynamics of the amorphous polymeric component. In addition, molecular weight and dispersion of POSS1 in the PS matrix are also main effect factors of T_g, which can explain why T_g of PS5 is lower than that of PS3.

3.8. Mechanical properties

The mechanical properties of PS/POSS1 nanocomposites are listed in Table 2. The simultaneous increase in tensile strength and elongation at break can obviously be attributed to a more efficient stress transfer mechanism between two components of hybrid composites. These phenomena might be distinctive feature of nanocomposites. Tensile strength of PS/POSS1 nanocomposites is increased with POSS1 content and reaches maximum 33.91 MPa when POSS1 content is up to 3 wt%, but tensile strength of PS5 is decreased as much as neat PS. The elongation at break is increased by 44% after addition of 1 wt% POSS1, and is decreased when the content of POSS1 exceeded 3 wt%, however, the value is still higher than that of the pure PS matrix. The increase trend of impact

Table 2
The mechanical properties of the pure PS and PS/POSS1 nanocomposites

Sample	Tensile strength (MPa)	Elongation at break (%)	Elastic modulus (MPa)	Impact strength (kJ/m^2)
PS0	26.70	5.05	540.10	48.45
PS1	32.10	7.29	565.43	79.65
PS3	33.91	6.61	566.61	90.06
PS5	26.65	5.68	534.72	47.73

strength of the PS/POSS nanocomposites with the POSS1 content is in agreement with that of tensile strength. The impact strength of PS3 is increased by 86% than that of neat PS. It is seldom reported that tensile strength, elongation at break and impact strength simultaneously obtained such high increase in traditional PS hybrids, such as PS/clay nonocomposites [10–12]. The effects of POSS1 content on the elastic modulus of PS/POSS1 nanocomposites, however, are not obvious. The improvement of mechanical properties can result from better adhesion, strong interaction between the POSS1 and PS, and molecular weight. The concentration of phase-separated POSS1 nanoparticals in the PS5 sample is drastically intensified so that the actual content within the amorphous polymer phase is lower than that in the PS3 sample. This relates the lowering of T_g and the lowering of the tensile strength with the reduced PS–POSS1 phase interaction.

3.9. Dynamic mechanical properties

The bending storage modulus E' vs. temperature curves for the neat PS and PS/POSS1 nanocomposites containing 3 and 5 wt% of POSS1 are shown in Fig. 9. The storage modulus reflects the elastic modulus of nanocomposites. In the glass state (temperature $< T_g$), the storage modulus E' of PS3 and PS5 are slightly lower than that of neat PS, but in rubbery state, the E' values of nanocomposites are higher than that of the neat PS. For example, the E' values of the neat PS and nanocomposites with 3 and 5 wt% POSS1 are 43.5, 248, 190 MPa, respectively, at 92 °C. The E' value of the composite with 3 wt% POSS1 is about five times higher than that of the neat PS. Fig. 10 shows the temperature dependence of tan δ of the PS/POSS1 nanocomposites. The loss factor tan δ is the ratio of the loss modulus to the storage modulus, and is very sensitive to the structural transformation of the materials. The tan δ peak also can be used to identify T_g of these nanocomposites, which shifted to high temperature as the tendency of T_g by DSC. It is seen that the T_g values are 94.19, 102.67 and 99.50 °C for PS0, PS3 and PS5, respectively, and T_g

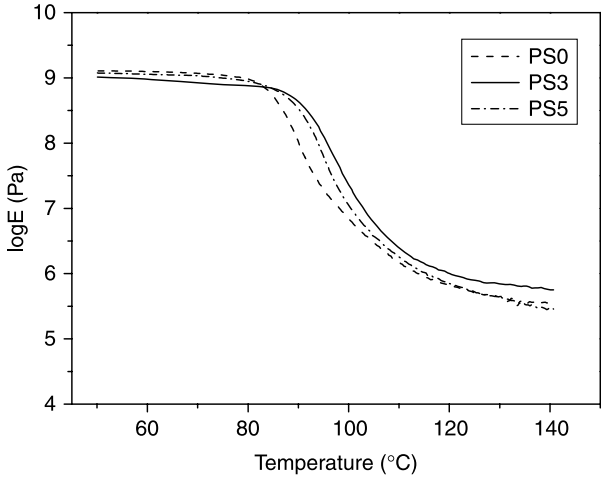

Fig. 9. Dynamic storage modulus for the neat PS and PS/POSS1 nanocomposites.

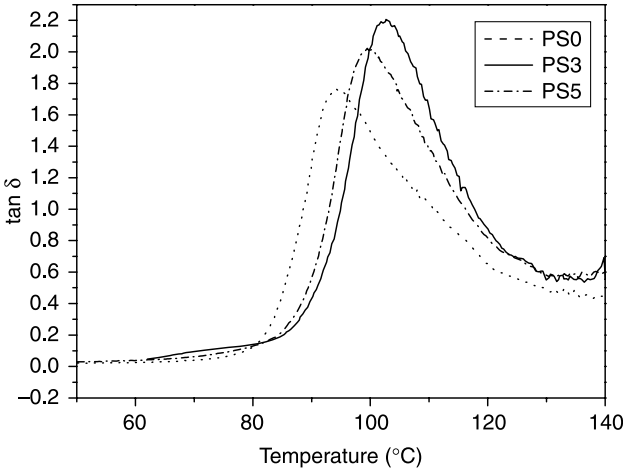

Fig. 10. DMA tan δ for the neat PS and PS/POSS1 nanocomposites.

of PS5 is not increased for further addition of POSS1 and decreases by 3 °C than that of PS3 in agreement with DSC result. In the glass state, the POSS1 has flexible effect on PS matrix, which is demonstrated by the impact strength increases in the PS/POSS1 nanocomposites. While the significant increase in T_g and rubbery state modulus suggest presence of the bulky and rigid particles retard the motion of the polymer chain and stiffen PS matrix due to strong interactions between the POSS1 and PS polymer chain. The T_g and storage modulus of PS5 is lower than that of PS3 because of the reduced dispersion at high concentration of particles and the low molecular weight of PS5.

4. Conclusion

Fc–CH=CH–C_6H_6–$(C_5H_9)_7Si_8O_{12}$ (POSS1, Fc: ferrocene) which contain both metal and double bond was firstly synthesized as a mixture of *E*/*Z* isomers. The POSS1 exhibits paramagnetic properties with a remnant magnetization of 0.035 emu/g and hysteresis coercive force (H_c) of 0 Oe at room temperature.

The POSS1-containing hybrids of polystyrene were prepared via bulk free radical polymerization. XRD, TEM and GPC data show that POSS1 is completely molecularly dispersed in PS when 1 wt% POSS1 is added, while a portion of the POSS1 is aggregated in the PS/POSS1 97/3 and 95/5 composites. Average molecular weight increases and M_w/M_n ratios have no apparent changes after addition of the POSS1 by GPC.

The thermal stability of PS/POSS1 nanocomposites has apparent improvement compared to pure PS by TGA and TMA. The temperature at the beginning of decomposition and deformation for PS and PS/POSS1 nanocomposites is increased with increase of POSS1 content. The glass transition behavior of the nanocomposites is investigated by means of DSC and DMTA. Compared with the pure PS, all the POSS-containing nanocomposites display higher T_g temperature. The DMA results show that all PS/POSS1 nanocomposites exhibit higher storage modulus (E') values (temperature $> T_g$) than

the pure PS, indicating the nanoreinforcement effect of POSS cage. The presence of the POSS1 also shows significant effects on the mechanical properties of PS. Tensile strength and impact strength of PS/POSS1 namocomposites are increased by 27 and 84.4%, respectively when POSS1 content is up to 3 wt%, and are both decreased as much as that of pure PS after addition of 5% POSS1. Only addition of 1% POSS1 results in 44.3% increase for the elongation at break. However, the presence of POSS1 has no apparent effect on elastic modulus of PS.

Acknowledgements

We gratefully acknowledge the financial support of National Science Foundation (grant no. CN20374007) and New Century Excellent Talent (NECT) and Key Project on Science and Technology of Ministry of Education (grant No.03023).

References

[1] Lichtenhan JD, Otonari YA, Carr MJ. Macromolecules 1995;28:8435.
[2] Lee A, Lichtenhan JD. J Appl Polym Sci 1999;73:1993.
[3] Haddad TS, Lichtenhan JD. Macromolecules 1996;29:7302.
[4] Romo-Uribe A, Mather PT, Haddad TS, Lichtenhan JD. J Polym Sci, Part B: Polym Phys 1998;36:1857.
[5] Li GZ, Wang L, Toghiani H, Daulton TL, Pittman Jr CU. Polymer 2002; 43:4167.
[6] Park C, Smith Jr JG, Connell JW, Lowther SE, Working DC, Siochi EJ. Polymer 2005;46:9694.
[7] Yei D-R, Kuo S-W, Fu H-K, Chang F-C. Polymer 2005;46:741.
[8] Xie W, Hwu JM, Jiang GJ. Polym Eng Sci 2003;43:214.
[9] Yei D-R, Kuo S-W, Fu H-K, Chang F-C. Polymer 2004;45:2633.
[10] Tseng C-R, Wu J-Y, Lee H-Y, Chang F-C. J Appl Polym Sci 2002;85: 1370.
[11] Su S, Wilkie CA. J Polym Sci, Part A: Polym Chem 2003;41:1124.
[12] Kin MH, Park CI, Choi WM, Lee JW, Lim JG, Park OO. J Appl Polym Sci 2004;92:2144.
[13] Lichtenhan JD, Otonari YA, Carr MJ. Macromolecules 1995;28:8435.
[14] Pyun J, Matyjaszewski K. Macromlecules 2000;33:217.
[15] Mather PT, Jeon HG, Romo-Uribe A. Macromolecules 1999;32:1194.
[16] Bharadwaj BK, Berry RJ, Farmer BL. Polymer 2000;41:7209.
[17] Jeon HG, Mather PT, Haddad TS. Polym Int 2000;49:453.
[18] Tsuchida A, Bolln C, Sernetz FG, Frey H, Mulhaupt R. Macromolecules 1997;30:2818.
[19] Zhang C, Babonneau F, Bonhomme C, Laine RM, Soles CL, Hristo, Yee AF. J Am Chem Soc 1998;120:8380.
[20] Lee A, Lichtenhan JD. Macromolecules 1998;31:4970.
[21] Liu Y, Zheng S, Nie K. Polymer 2005;46:12016.
[22] Ni Y, Zheng S, Nie K. Polymer 2004;45:5557.
[23] Lichtenhan JD, Vu NQ, Carter JA, Gilman JW, Feher FJ. Macromolecules 1993;26:2141.
[24] Huang J-C, He C-B, Xiao Y, Mya KY, Dai J, Siow YP. Polymer 2003;44: 4491.
[25] Voronkov MG, Lavret'yev V. Top Curr Chem 1982;102:199.
[26] Lorenz V, Fischer A, Edelmann FT. Inorg Chem Commun 2000;3:292.
[27] Lorenz V, Fischer A, Edelmann FT. J Organomet Chem 2002;647:245.
[28] Edelmann FT, Gießmanm S, Fischer A. Inorg Chem Commun 2000;3: 658–61.
[29] Harrison PG. J Organomet Chem 1997;542:141.
[30] Hay MT, Hainaut BJ, Geib SJ. Inorg Chem Commun 2003;6:431.
[31] Shapley PA, Stuart Bigham W, Hay MT. Inorg Chim Acta 2003;345:255.
[32] Moran M, Casado CM, Cuadrado I. Organometallics 1993;12:4327.
[33] Casado CM, Cuadrado I, Moran M, Alonso B. Organometallics 1995;14: 2618.
[34] Losada J, Garcia MP, Cuadrado O, Alonso B, Gonzalez B. J Organomet Chem 2004;689:2799.
[35] Wada K, Itayama N, Watanabe N, Bundo M, Kondo T, Mitsudo T-A. Organometallics 2004;23:5824.
[36] Feher FJ, Budzlchowskl TA, Blanskl RL, Weller KJ, Ziller JW. Organometallics 1991;10:2526.
[37] Wahab MA, Kim II, Ha CS. Polymer 2003;44:4705.
[38] Zheng L, Kasi RM, Farris RJ, Bryan Coughlin E. J Polym Sci, Part A: Polym Chem 2002;40:885.
[39] Kalogeras IM. Acta Mater 2005;53:1621.
[40] Alcoutlabi M, McKenna GB. J Phys: Condens Matter 2005;17:R461.
[41] Fu BX, Gelfer MY, Hsiao BS, Phillips S. Polymer 2003;44:1499.